Title: Bur1-driven G1-to-S phase transition induces hydroxyurea sensitivity in yeast checkpoint mutants

Authors: Stefany Cristine Rodrigues da Silva[1] and Francisco Meirelles Bastos de Oliveira[1, #]

Authors affiliation: [1] Instituto de Biofísica Carlos Chagas Filho, Universidade Federal do Rio de Janeiro, Rio de Janeiro, Brazil

Full mailing address: Instituto de Biofísica Carlos Chagas Filho, Universidade Federal do Rio de Janeiro, Av. Carlos Chagas Filho 373, Cidade Universitária, 21941-902, Rio de Janeiro, RJ, Brazil.

[#] Email address for corresponding author: francisco@biof.ufrj.br

Short running head: Bur1 induces HU sensitivity in checkpoint kinase mutants

Keywords: Bur1, cell cycle, hydroxyurea, checkpoint kinase, replication stress, *Saccharomyces cerevisiae*.

Abstract

In *Saccharomyces cerevisiae*, the cyclin-dependent kinase Bur1 is known for its role in promoting transcription elongation and histone modifications, thereby regulating gene expression. In this study, we investigated the genetic interactions between a hypomorphic *BUR1* allele (*bur1-107*) and null mutants of the checkpoint kinases Mec1 and Rad53. Our findings show that the *bur1-107* allele suppresses hydroxyurea (HU) sensitivity in *mec1* and *rad53* mutants, indicating that Bur1 activity may be detrimental in the absence of functional checkpoint signaling. Additionally, the *bur1-107* mutation delays the G1-to-S phase transition, indicating a key role for Bur1 in cell cycle progression. Notably, *bur1-107* reduces γ-H2A accumulation, facilitates S-phase resumption, and supresses the sub-G1 population in HU-treated *mec1* mutants. These findings suggest that Bur1-driven G1-to-S phase progression exacerbates DNA damage and cell death in checkpoint-deficient cells exposed to HU. This study highlights a novel role for Bur1 in modulating the cellular response to replication stress in checkpoint-compromised cells.

Introduction

During DNA replication, depletion of deoxyribonucleotide triphosphates (dNTPs) can cause replication fork stalling and expose single-stranded DNA (ssDNA), leading to replication stress (RS) (Sogo et al. 2002; Poli et al. 2012). To counteract RS, eukaryotic cells activate the replication stress response (RSR), a set of cellular processes aimed to protect stalled replication forks. Failure to establish an effective RSR can lead to replication fork collapse and increased DNA damage, driving genome instability (Zeman and Cimprich 2014; Saldivar et al. 2017).

In *Saccharomyces cerevisiae*, RSR signaling is mediated by the apical kinase Mec1 and the downstream kinase Rad53, functional homologues of human ATR and Chk1, respectively (Pardo et al. 2017; Lanz et al. 2019; Cussiol et al. 2020). While these kinases were historically known as checkpoint kinases for their role in regulating cell cycle progression (Allen et al. 1994; Weinert et al. 1994), they also perform additional functions. Mec1 and Rad53 suppress late origin firing, stabilize replication forks, and increase dNTP levels by activating ribonucleotide reductase (RNR) genes and degrading the RNR inhibitor Sml1 (Huang et al. 1998; Santocanale and Diffley 1998; Shirahige et al. 1998; Zhao et al. 1998; Lopes et al. 2001; Tercero et al. 2003).

In *S. cerevisiae*, *BUR1* encodes a cyclin-dependent protein kinase homologous to human CDK9 (Yao et al. 2000). Along with its cyclin partner Bur2, Bur1 phosphorylates the C-terminal domain of RNA polymerase II and the transcription elongation factor Spt5, thereby facilitating transcriptional elongation (Murray et al. 2001; Liu et al. 2009). Additionally, Bur1 is involved in co-transcriptional histone modifications, including the

69 monoubiquitination of histone H2B and the mono- and trimethylation of histone H3
70 (Laribee et al. 2005; Wood et al. 2005; Chu et al. 2006). Through these mechanisms,
71 the Bur1-Bur2 complex regulates the expression of a broad range of genes (Laribee et
72 al. 2005).

73 Growing evidence suggests a functional interplay between the Bur1-Bur2 complex and
74 the RSR pathway. Bur1 was found to physically interact with Rfa1, a subunit of the
75 replication protein A (RPA) complex and a key sensor of RS (Clausing et al. 2010).
76 Bur2-deficient cells exhibits sensitivity to hydroxyurea (HU), an RNR inhibitor that
77 depletes dNTPs and is commonly used to induce RS (Lau et al. 2010). Additionally, HU-
78 treated *bur1* mutants display an accumulation of Rad52 foci, suggesting that Bur1 is
79 involved in preventing the colpase of stalled replication forks (Clausing et al. 2010).

80 To further explore Bur1's role in the RSR we conducted a genetic interaction analysis by
81 combining a hypomorphic mutant of *BUR1* (*bur1-107*) with null alleles of *MEC1* or
82 *RAD53*. Our study shows that the *bur1-107* mutantion alleviates the HU sensitivity in
83 *mec1* and *rad53* mutants. Additionally, we found that the *bur1-107* mutant delays the
84 transition from G1 to S-phase. Notably, *bur1-107* reduces γ-H2A accumulation,
85 facilitates S-phase resumption and supresses the sub-G1 population in HU-treated
86 *mec1*Δ cells. These findings suggest that, in the absence of a functional checkpoint,
87 Bur1 may have a detrimental effect, potentially by driving an inappropriate transition
88 from G1 to S-phase.
89
90
91

92 **Materials and methods**

93 **Strains and plasmids**

94 Unless otherwise noted, all strains are derived from the S288C background. Gene
95 deletions were achieved by replacing the endogenous allele with drug-resistance
96 cassettes or auxotrophic markers, generated by PCR (Longtine et al. 1998). Yeast
97 transformations were performed using the lithium acetate method (Gietz 2014), and
98 successful knockouts were confirmed by PCR with specific primers. To construct the
99 *bur1-107* strain, the *BUR1* open reading frame and a 50 bp upstream region were
100 cloned into the pFA6a-kanMX6 vector using *PacI* and *AscI*. Site-directed mutagenesis
101 introduced the G52R and G222N mutations. A 466 bp downstream region of *BUR1* was
102 then cloned into the plasmid using *PmeI* and *SpeI*. The *bur1-107* construct was excised
103 with *PacI* and *SpeI* and integrated into the *BUR1* locus in a diploid strain. After
104 sporulation, haploid strains carrying the *bur1-107* allele were isolated by tetrad
105 dissection and confirmed by PCR and kanMX6 marker selection. The same procedure
106 was used to generate isogenic strains with the wild-type *BUR1* allele.
107

108 **Cell growth, media, and synchronization**

109 Unless stated otherwise, cells were cultured in YPD medium (1% yeast extract, 2%
110 peptone, 2% dextrose) at 30°C to logarithmic phase. For synchronization, *bar1*Δ cells
111 were treated with α-factor (50 ng/mL for *bar1*Δ strains, 5 µg/mL for *bar1*Δ *mec1*Δ or
112 *bar1*Δ *rad53*Δ strains) for 2,5 hours (Amberg et al. 2006). Cells were then released from
113 G1 arrest by centrifugation and resuspended in fresh medium containing 50 µg/mL

114 pronase, with or without HU. The specific HU concentrations used are indicated in the
115 corresponding figures and figure legends.
116
117 **Drug sensitivity assays**

118 Overnight cultures were inoculated in YPD medium to an initial OD_{600} of 0.1 and grown
119 to mid-log phase. Cultures were then adjusted to an OD_{600} of 1.0, and five-fold serial
120 dilutions were spotted onto plates with or without HU. Plates were incubated at 30°C for
121 1–3 days, then inspected for growth and photographed. For drug sensitivity assays with
122 6-azauracil (6AU), pRS316-bearing cells were cultured in synthetic complete medium
123 lacking uracil (SC-URA). The specific HU and 6AU concentrations used are indicated in
124 the corresponding figures and figure legends.
125
126 **Flow cytometry**

127 A total of 5×10^6 yeast cells were harvested, washed with distilled water, and sonicated
128 (10 seconds at 20% amplitude) to disperse clumps. Cells were fixed in 1 mL of 70%
129 ethanol overnight at 4°C. After fixation, cells were centrifuged, ethanol removed, and
130 pellets resuspended in 50 mM sodium citrate buffer (pH 7.2). The samples were treated
131 with 250 µg/mL RNase A at 37°C overnight, followed by 2 hours with 500 µg/mL
132 proteinase K at 50°C. SYTOX™ Green (0.25 µL; Thermo Fisher Scientific) was then
133 added, and samples were incubated for 1 hour at room temperature in the dark. Data
134 acquisition was performed using a BD FACSCalibur™ flow cytometer.
135
136 **Western blotting**

137 Yeast cultures were grown to mid-log phase and treated as described in the figure
138 legends. Cells were harvested and washed with TE buffer (pH 8.0) containing 1 mM
139 PMSF. Pellets were lysed by bead beating with 0.5-mm glass beads for three 5-minute
140 cycles (1-minute rest between cycles) at 4°C in lysis buffer (150 mM NaCl, 50 mM Tris
141 pH 8.0, 5 mM EDTA, 0.2% NP-40) with cOmplete™ EDTA-free protease inhibitor
142 cocktail (Roche), PhosStop™ phosphatase inhibitor cocktail (Roche), and 1 mM PMSF.
143 Lysates were boiled in Laemmli buffer and subjected to SDS-PAGE. Proteins were
144 transferred to PVDF membranes by wet transfer and incubated with specific primary
145 antibodies: anti-γ-H2A (ab15083, Abcam, 1:1,000), anti-Rad53 (ab166859, Abcam,
146 1:5,000), and anti-PGK1 (459250, Invitrogen, 1:5,000). After primary antibody
147 incubation, membranes were treated with ECL HRP-linked secondary antibodies (anti-
148 mouse NA931, Cytiva, 1:5,000; anti-rabbit NA934, Cytiva, 1:5,000). Blots were
149 developed with ECL™ Prime reagent (Amersham) and imaged using an Amershan™
150 Imager 600.
151
152
153
154
155
156
157
158
159

Results

Bur1 exacerbates HU sensitivity in *mec1* and *rad53* mutants

To further investigate Bur1's role in RSR, we conducted a pairwise genetic interaction analysis between *BUR1* and the checkpoint kinase genes *MEC1* and *RAD53*. Given that *BUR1* is essential, we used the hypomorphic *bur1-107* mutant, which contains two amino acid substitutions: G52R at the N-terminus and G222N within the activation segment of the kinase domain (Fig. 1a) (Clausing et al. 2010).

The *bur1-107* mutant showed increased sensitivity to 6-azauracil (6AU), an inhibitor of GTP and UTP synthesis (Fig. 1b). While reduced GTP and UTP levels are not lethal to wild-type cells, they significantly increase sensitivity in conjunction with mutations that impair transcriptional elongation (Exinger and Lacroute 1992). Additionally, we confirmed that the *bur2*Δ mutant is also sensitive to 6AU, further supporting the role of the Bur1-Bur2 complex in facilitating transcription elongation (Fig. 1b).

Since *MEC1* and *RAD53* are essential, the *mec1*Δ and *rad53*Δ mutants used in the genetic interaction assays were generated in a *sml1*Δ background (Zhao et al. 1998). Notably, the *bur1-107* mutant partially suppressed the sensitivity of both *mec1*Δ *sml1*Δ and *rad53*Δ *sml1*Δ cells to low doses of HU (Fig. 2a). Similarly, the deletion of *BUR2* also alleviated HU sensitivity in *mec1*Δ *sml1*Δ cells (Supplementary Fig. S1). These findings suggest that, in the absence of a functional checkpoint signaling, the Bur1-Bur2 complex exacerbates the detrimental effects of HU treatment.

To evaluate the impact of the *bur1-107* mutation on the viability of *mec1*Δ *sml1*Δ or *rad53*Δ *sml1*Δ mutants exposed to HU during a single round of DNA replication, cells

182 were synchronized in G1 phase using α-factor and subsequently released into S-phase
183 in the presence of 200 mM HU for two hours. As shown in Fig. 2b and c, *bur1-107*
184 partially restored viability in *mec1*Δ *sml1*Δ and *rad53*Δ *sml1*Δ mutants after two hours of
185 HU exposure.

186 Next, we questioned whether *bur1-107* would be sufficient to bypass the essential
187 functions of *MEC1* or *RAD53*. Diploid strains heterozygous for *bur1-107* and either
188 *mec1* or *rad53* alleles were generated, and spore viability was assessed following
189 tetrad dissection. As expected, *mec1*Δ and *rad53*Δ spores were inviable and failed to
190 form colonies (Fig. 2d). Although *bur1-107* spores grew to nearly wild-type size, no
191 colony formation was observed for *bur1-107 mec1*Δ or *bur1-107 rad53*Δ spores. These
192 results suggest that, unlike *sml1*Δ, *bur1-107* cannot compensate for the loss of *MEC1* or
193 *RAD53*.
194

195 ***bur1-107* delays the transition from G1 to S-phase independently of Mec1**

196 Throughout this study, we noted that the *bur1-107* mutant exhibited slower growth
197 compared to wild-type cells (Supplementary Fig. S2). This is consistent with previous
198 findings showing that Bur1-deficient cells undergo an extended G1 phase (Jin et al.
199 2022). To assess whether the *bur1-107* mutant is defective in the G1-to-S phase
200 transition, cells were synchronized in G1, released into S-phase, and DNA content was
201 analyzed by flow cytometry (Fig. 3a). To prevent complete DNA replication stalling,
202 experiments were conducted with 20 mM of HU (Fig. 3c). As expected, *mec1*Δ *sml1*Δ
203 cells progressed through S phase slightly faster than wild-type cells (*sml1*Δ). However,
204 despite their accelerated progression, *mec1*Δ *sml1*Δ cells were unable to complete DNA

205 replication, even 120 minutes after release from α-factor arrest. Interestingly, *bur1-107*
206 *sml1*Δ and *bur1-107 mec1*Δ *sml1*Δ cells exhibited a more pronounced delay in G1/S
207 progression compared to *mec1*Δ *sml1*Δ cells, both with or without HU (Fig. 3b and c).
208 Consistent with its role in promoting the G1/S transition, *bur1-107 sml1*Δ and *bur1-107*
209 *mec1*Δ *sml1*Δ mutants showed a delay in bud formation compared to *mec1*Δ *sml1*Δ
210 (Fig. 3d). These data suggest that Bur1 is required for cell cycle progression from G1 to
211 S-phase, independently of Mec1.
212

213 ***BUR1 increases DNA damage and impairs the resumption of S-phase in mec1***
214 ***mutants treated with HU***

215 To further investigate the effect of Bur1 in *mec1*Δ *sml1*Δ cells, we evaluated the impact
216 of the *bur1-107* mutation on DNA damage signaling. Cells were synchronized in G1 and
217 then released into S-phase with 200 mM of HU for up to 120 minutes (Fig. 4a, b and
218 Supplementary Fig. S3). Consistent with previous studies, Rad53 activation was
219 observed at 30 and 60 minutes in wild-type cells (*sml1*Δ), while no increase in γ-H2A
220 signal was detected (Puddu et al. 2011). In contrast, *mec1*Δ *sml1*Δ cells showed γ-H2A
221 accumulation and reduced Rad53 activation. Intriguingly, *bur1-107 mec1*Δ *sml1*Δ cells
222 displayed a significant decrease in Rad53 phosphorylation and γ-H2A signal compared
223 to *mec1*Δ *sml1*Δ cells. These findings demonstrate that, in *mec1*Δ *sml1*Δ cells exposed
224 to HU, Bur1 exacerbates RS and promotes DNA damage.

225 To determine whether Bur1 influences the resumption of S-phase in HU-treated *mec1*Δ
226 *sml1*Δ cells, we analyzed cell cycle progression following a two-hour HU-induced
227 replication block (Fig. 4a and c). *bur1-107 sml1*Δ cells initially exhibit a delay in S-phase

228 progression 30 minutes after HU removal but resumed replication between 90 and 120
229 minutes. In contrast, *mec1*Δ *sml1*Δ cells showed a pronounced defect in replication
230 resumption, failing to reach the 2C DNA content peak even 180 minutes post-HU
231 removal. Consistent with the observed lethality in *mec1*Δ *sml1*Δ cells treated with HU
232 (Fig. 2c and d), a sub-G1 population was detected at 180 minutes after HU removal
233 (Fig. 4c, red brackets). Interestingly, although *bur1-107 mec1*Δ *sml1*Δ mutants
234 progressed slowly through S-phase, a subset of these cells reached the 2C DNA
235 content peak at 120 minutes post-HU release. Notably, by 180 minutes after HU
236 removal, the *bur1-107 mec1*Δ *sml1*Δ mutant exhibited a lower percentage of cells in
237 sub-G1 compared to *mec1*Δ *sml1*Δ cells (Fig. 4d). These findings suggest that Bur1
238 exacerbates DNA replication defects in *mec1*Δ *sml1*Δ cells following HU treatment,
239 resulting in increased DNA damage and cell death.
240
241
242
243
244
245
246
247
248
249
250

251 **Discussion**

252 Growing evidence suggests a functional interplay between the Bur1-Bur2 complex and
253 the RSR pathway. Our study reveals a genetic interaction between *BUR1* and the
254 genes encoding the checkpoint signaling kinases Mec1 and Rad53. Notably, we
255 observed that the *bur1-107* mutant alleviates HU sensitivity in *mec1*Δ *sml1*Δ and *rad53*Δ
256 *sml1*Δ cells. These findings imply that in the absence of functional checkpoint signaling,
257 Bur1 may have a detrimental impact on cells treated with HU.

258 Bur1 was initially identified as a CDC28/cdc2-related kinase essencial for the adaptative
259 response to pheromone-induced G1 arrest (Irie et al. 1991). Although the precise
260 mechanism is not fully understood, it has been proposed that Bur1 aids the transition
261 from G1 phase by activating G1 cyclins. Supporting this hypothesis, Bur1-deficient cells
262 show increased retention of nuclear Whi5, a known G1 marker (Jin et al. 2022).
263 Consistently, we observed that the *bur1-107* mutant exhibits a prolonged doubling time
264 and delayed progression from G1 to S-phase.

265 The Bur1-Bur2 complex is critical for facilitating transcription elongation, thereby
266 regulating the expression of a wide range of genes. In particular, the *bur1-107* mutation
267 impairs transcription elongation and results in decreased mRNA levels of cyclins Cln2,
268 Clb1, and Clb6 (Clausing et al. 2010). This suggests that *bur1-107* might also impact
269 the expression of other genes essencial for cell cycle regulation, particularly those
270 involved in the G1 to S-phase transition. Additionaly, It is possible that Bur1 directly
271 phosphorylates substrates that promote the G1 to S-phase transition, independently of
272 its role in transcriptional regulation.

273 Our findings reveal that the *bur1-107* mutation supresses the lethality of *mec1*Δ *sml1*Δ
274 cells and facilitates the resumption of S-phase following a two-hour replication block
275 with HU. Adittionally, the *bur1-107* mutation significantly reduces the accumulation of γ-
276 H2A in HU-treated *mec1*Δ *sml1*Δ cells. It is reasonable to hypothesize that by delaying
277 the G1 to S-phase transition, the *bur1-107* mutation alleviates the detrimental effects of
278 HU-induced RS in *mec1*Δ *sml1*Δ cells. Indeed, the observed lethality in *mec1* and *rad53*
279 mutants is largely attributed to a Cdc28-dependent function during G1 phase.
280 Consistently, Cdc28-defective strains supress the HU-induced lethality in *mec1*Δ *sml1*Δ
281 and *rad53*Δ *sml1*Δ cells (Manfrini et al. 2012). Similarly, a *cln2*Δ mutant, which delays
282 the G1-to-S phase transition, also suppresses the requirement for Mec1 and Rad53
283 during an unperturbed cell cycle (Manfrini et al. 2012). Although the precise mechanism
284 of suppression remains unclear, it has been proposed that delaying the G1-to-S phase
285 transition allows *mec1* and *rad53* mutants additional time to accumulate sufficient
286 dNTPs for DNA replication, thereby alleviating RS (Vallen and Cross 1999). Our data
287 support this model, showing that in *mec1*Δ cells, the downregulation of *BUR1*, in
288 combination with *SML1* inactivation, suppresses HU sensitivity, likely by increasing
289 dNTP pools and thus reducing the dependence on Mec1 for checkpoint activation.

290 Interestingly, while the Bur1-Bur2 complex seems to exacerbate stress in checkpoint
291 kinase-deficient strains treated with low doses of HU, the *bur1-107* and *bur2*Δ mutants
292 exhibit increased sensitivity to higher HU concentrations (Supplementary Fig. S4).
293 Consistent with this observation, *bur1-107* exhibit an increase in Rad52 foci in HU-
294 treated cells, suggesting that the Bur1-Bur2 complex may regulate additional processes

295 crucial for protecting cells from the detrimental effects of prolonged exposure to high HU
296 doses (Clausing et al. 2010).

297 In human cells, the Bur1 homologue, CDK9, is crucial for maintaining genome stability.
298 Depletion of CDK9 impairs cell cycle recovery in response to RS and induces
299 spontaneous DNA damage during replication (Yu et al. 2010). Additionaly, CDK9-
300 deficient cells exhibit altered γ-H2AX foci dynamics and reduced efficiency in
301 homologous recombination repair following ionizing radiation (Nepomuceno et al. 2017).

302 Here, we demonstrate that despite evidence supporting a protective role for Bur1 during
303 RS, it can exert a detrimental effect in cells with compromised cell cycle checkpoints.
304 Specifically, Bur1-driven G1-to-S phase transition exacerbates RS and promotes cell
305 death in *mec1* mutants exposed to HU. To fully elucidate this dual role of Bur1, future
306 studies should focus on systematically identifying its transcriptional targets and
307 phosphorylation substrates, along with investigating their precise roles in regulating cell
308 cycle progression and the cellular response to RS.
309
310
311
312
313
314
315
316
317

318 **Data availability**

319 Strains and plasmids used in this study are available upon request. Supplementary
320 Tables 1 and 2 provide detailed lists of the yeast strains and plasmids utilized.
321 Supplementary Figures S1 and S2 include additional data supporting Figures 2 and 3,
322 respectively, while Supplementary Figures S3 and S4 offer supplementary data
323 supporting Figure 4 and the discussion section, respectively.
324
325
326
327
328
329
330
331
332
333
334
335
336
337
338
339

Acknowledgments

We thank Marcelo Fantappié, Ronaldo Mohana and Marcelo de Pádula for providing access to their laboratory and equipment. We also thank Claudio Masuda, José Renato Cussiol, Marcelo Alex de Carvalho and Thales Nepomuceno for their valuable comments and suggestions and Patricia Abrão Possik and Marcus Smolka for sharing reagents. Our appreciation goes to Anderson Amarante and Karina Lani Silva for their technical support. Additionally, we acknowledge the Plataforma de Sequenciamento de DNA (PSEQDNA-UFRJ) for DNA sequencing and the Plataforma de Imuno Análise (PIA-UFRJ) for flow cytometry analysis of DNA content.

Funding

This work was supported by a grant from FAPERJ (No. E-26/010.002187/2019) and CNPq (MCTI-FNDCT No. 18/2021). SCRdS received a PhD fellowship from CNPq (141014/2021-0).

Conflicts of interest

The author(s) declare no conflict of interest.

Authors contribution

FMBdO conceived the project, FMBdO and SCRdS wrote the paper, designed the experiments and analyzed the data. SCRdS performed the experiments.

432 **Literature cited**

433 Allen JB, Zhou Z, Siede W, Friedberg EC, Elledge SJ. 1994. The SAD1/RAD53 protein
434 kinase controls multiple checkpoints and DNA damage-induced transcription in yeast.
435 Genes Dev. 8(20):2401–2415. doi:10.1101/gad.8.20.2401.
436 Amberg DC, Burke DJ, Strathern JN. 2006. Inducing Yeast Cell Synchrony: α-Factor
437 Arrest Using *bar1* Mutants. Cold Spring Harb Protoc. 2006(1):pdb.prot4173.
438 doi:10.1101/pdb.prot4173.
439 Chu Y, Sutton A, Sternglanz R, Prelich G. 2006. The Bur1 Cyclin-Dependent Protein
440 Kinase Is Required for the Normal Pattern of Histone Methylation by Set2. Mol Cell Biol.
441 26(8):3029–3038. doi:10.1128/mcb.26.8.3029-3038.2006.
442 Clausing E, Mayer A, Chanarat S, Müller B, Germann SM, Cramer P, Lisby M, Strässer
443 K. 2010. The transcription elongation factor Bur1-Bur2 interacts with replication protein
444 A and maintains genome stability during replication stress. Journal of Biological
445 Chemistry. 285(53):41665–41674. doi:10.1074/jbc.M110.193292.
446 Cussiol JRR, Soares BL, Oliveira FMB de. 2020. From yeast to humans: Understanding
447 the biology of DNA Damage Response (DDR) kinases. Genet Mol Biol. 43(1 suppl 1).
448 doi:10.1590/1678-4685-gmb-2019-0071.
449 Exinger F, Lacroute F. 1992. 6-Azauracil inhibition of GTP biosynthesis in
450 Saccharomyces cerevisiae. Curr Genet. 22(1):9–11. doi:10.1007/BF00351735.
451 Gietz RD. 2014. Yeast Transformation by the LiAc/SS Carrier DNA/PEG Method. p. 1–
452 12.

453 Huang M, Zhou Z, Elledge SJ. 1998. The DNA Replication and Damage Checkpoint
454 Pathways Induce Transcription by Inhibition of the Crt1 Repressor. Cell. 94(5):595–605.
455 doi:10.1016/S0092-8674(00)81601-3.
456 Irie K, Nomoto S, Miyajima I, Matsumoto K. 1991. SGV1 encodes a CDC28/cdc2-
457 related kinase required for a Gα subunit-mediated adaptive response to pheromone in
458 S. cerevisiae. Cell. 65(5):785–795. doi:10.1016/0092-8674(91)90386-D.
459 Jin Y, Jin N, Oikawa Y, Benyair R, Koizumi M, Wilson TE, Ohsumi Y, Weisman LS.
460 2022. Bur1 functions with TORC1 for vacuole-mediated cell cycle progression. EMBO
461 Rep. 23(4). doi:10.15252/embr.202153477.
462 Lanz MC, Dibitetto D, Smolka MB. 2019. DNA damage kinase signaling: checkpoint and
463 repair at 30 years. EMBO J. 38(18):e101801. doi:10.15252/embj.2019101801 PMID -
464 31393028.
465 Laribee RN, Krogan NJ, Xiao T, Shibata Y, Hughes TR, Greenblatt JF, Strahl BD. 2005.
466 BUR kinase selectively regulates H3 K4 trimethylation and H2B ubiquitylation through
467 recruitment of the PAF elongation complex. Current Biology. 15(16):1487–1493.
468 doi:10.1016/j.cub.2005.07.028.
469 Lau NC, Mulder KW, Brenkman AB, Mohammed S, van den Broek NJF, Heck AJR,
470 Timmers HTM. 2010. Phosphorylation of Not4p functions parallel to BUR2 to regulate
471 resistance to cellular stresses in saccharomyces cerevisiae. PLoS One. 5(4).
472 doi:10.1371/journal.pone.0009864.
473 Liu Y, Warfield L, Zhang C, Luo J, Allen J, Lang WH, Ranish J, Shokat KM, Hahn S.
474 2009. Phosphorylation of the Transcription Elongation Factor Spt5 by Yeast Bur1

475 Kinase Stimulates Recruitment of the PAF Complex. Mol Cell Biol. 29(17):4852–4863.
476 doi:10.1128/mcb.00609-09.
477 Longtine MS, McKenzie A, Demarini DJ, Shah NG, Wach A, Brachat A, Philippsen P,
478 Pringle JR. 1998. Additional modules for versatile and economical PCR-based gene
479 deletion and modification in Saccharomyces cerevisiae. Yeast. 14(10):953–961.
480 doi:10.1002/(SICI)1097-0061(199807)14:10<953::AID-YEA293>3.0.CO;2-U.
481 Lopes M, Cotta-Ramusino C, Pellicioli A, Liberi G, Plevani P, Muzi-Falconi M, Newlon
482 CS, Foiani M. 2001. The DNA replication checkpoint response stabilizes stalled
483 replication forks. Nature. 412(6846):557–561. doi:10.1038/35087613.
484 Malumbres M. 2014. Cyclin-dependent kinases. Genome Biol. 15(6):122.
485 doi:10.1186/gb4184.
486 Manfrini N, Gobbini E, Baldo V, Trovesi C, Lucchini G, Longhese MP. 2012. G 1 /S and
487 G 2 /M Cyclin-Dependent Kinase Activities Commit Cells to Death in the Absence of the
488 S-Phase Checkpoint . Mol Cell Biol. 32(24):4971–4985. doi:10.1128/mcb.00956-12.
489 Murray S, Udupa R, Yao S, Hartzog G, Prelich G. 2001. Phosphorylation of the RNA
490 Polymerase II Carboxy-Terminal Domain by the Bur1 Cyclin-Dependent Kinase. Mol
491 Cell Biol. 21(13):4089–4096. doi:10.1128/mcb.21.13.4089-4096.2001.
492 Nepomuceno TC, Fernandes VC, Gomes TT, Carvalho RS, Suarez-Kurtz G, Monteiro
493 AN, Carvalho MA. 2017. BRCA1 recruitment to damaged DNA sites is dependent on
494 CDK9. Cell Cycle. 16(7):665–672. doi:10.1080/15384101.2017.1295177.
495 Pardo B, Crabbé L, Pasero P. 2017. Signaling pathways of replication stress in yeast.
496 FEMS Yeast Res. 17(2). doi:10.1093/femsyr/fow101.

497 Poli J, Tsaponina O, Crabbé L, Keszthelyi A, Pantesco V, Chabes A, Lengronne A,
498 Pasero P. 2012. dNTP pools determine fork progression and origin usage under
499 replication stress. EMBO J. 31(4):883–894. doi:10.1038/emboj.2011.470.
500 Puddu F, Piergiovanni G, Plevani P, Muzi-Falconi M. 2011. Sensing of Replication
501 Stress and Mec1 Activation Act through Two Independent Pathways Involving the 9-1-1
502 Complex and DNA Polymerase ε. PLoS Genet. 7(3):e1002022.
503 doi:10.1371/journal.pgen.1002022.
504 Saldivar JC, Cortez D, Cimprich KA. 2017. The essential kinase ATR: ensuring faithful
505 duplication of a challenging genome. Nat Rev Mol Cell Biol. 18(10):622–636.
506 doi:10.1038/nrm.2017.67.
507 Santocanale C, Diffley JFX. 1998. A Mec1- and Rad53-dependent checkpoint controls
508 late-firing origins of DNA replication. Nature. 395(6702):615–618. doi:10.1038/27001.
509 Shirahige K, Hori Y, Shiraishi K, Yamashita M, Takahashi K, Obuse C, Tsurimoto T,
510 Yoshikawa H. 1998. Regulation of DNA-replication origins during cell-cycle progression.
511 Nature. 395(6702):618–621. doi:10.1038/27007.
512 Sogo JM, Lopes M, Foiani M. 2002. Fork Reversal and ssDNA Accumulation at Stalled
513 Replication Forks Owing to Checkpoint Defects. Science (1979). 297(5581):599–602.
514 doi:10.1126/science.1074023.
515 Tercero JA, Longhese MP, Diffley JFX. 2003. A Central Role for DNA Replication Forks
516 in Checkpoint Activation and Response. Mol Cell. 11(5):1323–1336.
517 doi:10.1016/S1097-2765(03)00169-2.

518 Vallen EA, Cross FR. 1999. Interaction Between the MEC1-Dependent DNA Synthesis
519 Checkpoint and G1 Cyclin Function in Saccharomyces cerevisiae. Genetics.
520 151(2):459–471. doi:10.1093/genetics/151.2.459.
521 Weinert TA, Kiser GL, Hartwell LH. 1994. Mitotic checkpoint genes in budding yeast and
522 the dependence of mitosis on DNA replication and repair. Genes Dev. 8.
523 doi:10.1101/gad.8.6.652.
524 Wood A, Schneider J, Dover J, Johnston M, Shilatifard A. 2005. The Bur1/Bur2 complex
525 is required for histone H2B monoubiquitination by Rad6/Bre1 and histone methylation
526 by COMPASS. Mol Cell. 20(4):589–599. doi:10.1016/j.molcel.2005.09.010.
527 Yao S, Neiman A, Prelich G. 2000. *BUR1* and *BUR2* Encode a Divergent Cyclin-
528 Dependent Kinase–Cyclin Complex Important for Transcription In Vivo. Mol Cell Biol.
529 20(19):7080–7087. doi:10.1128/MCB.20.19.7080-7087.2000.
530 Yu DS, Zhao R, Hsu EL, Cayer J, Ye F, Guo Y, Shyr Y, Cortez D. 2010. Cyclin-
531 dependent kinase 9-cyclin K functions in the replication stress response. EMBO Rep.
532 11(11):876–882. doi:10.1038/embor.2010.153.
533 Zeman MK, Cimprich KA. 2014. Causes and consequences of replication stress. Nat
534 Cell Biol. 16(1):2–9. doi:10.1038/ncb2897 PMID - 24366029.
535 Zhao X, Muller EGD, Rothstein R. 1998. A Suppressor of Two Essential Checkpoint
536 Genes Identifies a Novel Protein that Negatively Affects dNTP Pools. Mol Cell.
537 2(3):329–340. doi:10.1016/S1097-2765(00)80277-4.
538
539
540

541 **Figure legends**

542 **Figure 1. *bur1-107* and *bur2* mutants are sensitive to 6AU.**

543 (a) Schematic of the *bur1-107* protein, highlighting the kinase domain and the G52R (N-
544 terminal) and G222N (kinase domain) mutations. The dotted line represents the amino
545 acid alignment of the activation segments between yeast transcription-related Cdks
546 Bur1, Ctk1, Kin28 and Srb10, spanning from the conserved DFG motif to the APE motif.
547 The hashtag marks the conserved phosphorylation-dependent threonine residue in the
548 T-loop (Malumbres 2014). The red arrow indicates the G222 residue mutated in *bur1-*
549 *107*. Numbers indicate amino acid positions, with asterisks marking conserved residues.
550 (b) Serial 1:5 dilutions of pRS316-bearing strains with the indicated genotypes were
551 spotted onto SC-URA plates with or without 6-azauracil (6AU). Plates were incubated at
552 30°C for 3 days.

553

554 **Figure 2. *bur1-107* improves viability of *mec1* and *rad53* mutants treated with HU.**

555 (a) and (b) Serial dilutions (1:5) of strains with indicated genotypes were spotted onto
556 YPD plates with or without hydroxyurea (HU). Plates were incubated at 30°C for 3 days.
557 (c) Strains with indicated genotypes were synchronized in G1 with α-factor, released
558 into YPD with pronase and 200 mM HU, and assessed for survival at indicated time
559 points by colony-forming units on fresh YPD plates. Plates were incubated at 30°C for 3
560 days. Data are the mean of at least three experiments. (d) Relative survival of S-phase
561 cells treated with 200 mM HU for 2 hours, compared to WT control. Data represent the
562 mean ± SEM from at least three independent experiments. *$P < 0.05$ (Student's
563 unpaired t-test). All strains used in the experiments shown in panels (a) to (d) carry the

564 *sml1*Δ mutation. (e) Meiotic tetrads from *MEC1*/*mec1*Δ *BUR1*/*bur1-107* or
565 *RAD53*/*rad53*Δ *BUR1*/*bur1-107* diploids were dissected on YPD and incubated at 30°C
566 for 3 days. WT and *bur1-107* single-mutant spores are indicated by squares and circles,
567 respectively.
568
569 **Figure 3. *bur1-107* delays the progression from G1 to S-phase.**
570 (a) Exponentially growing asynchronous cells were arrested in G1 with α-factor for 2,5
571 hours, then released into YPD at 25°C, either (b) without or (c) with 20 mM HU. DNA
572 content was analyzed by flow cytometry at the indicated time points. (d) Exponentially
573 growing strains with the indicated genotypes were arrested in G1 with α-factor for 2,5
574 hours and then released into YPD with pronase and 20 mM HU at 25°C. Budding index
575 was measured at the specified time points to monitor cell cycle progression. All strains
576 carry the *sml1*Δ mutation.
577
578 **Figure 4. *bur1-107* supresses DNA damage signaling and facilitates the**
579 **resumption of S-phase in HU-treated *mec1* mutants.**
580 (a) Exponentially growing asynchronous cells were arrested in G1 phase with α-factor
581 for 2,5 hours, followed by release into YPD containing 200 mM HU for an additional 2
582 hours. After HU treatment, cells were released into fresh YPD and incubated for 3 hours
583 at 30°C. (b) Samples were collected at the specified time points post-release from α-
584 factor for Western blot analysis to detect γ-H2A and Rad53. (c) DNA content was
585 analyzed by flow cytometry at the indicated time points. Red lines indicate sub-G1
586 populations. (d) Percentage of cells in sub-G1 phase at 180 minutes post-HU release,

587 relative to total cell cycle phases. Data represent the mean ± SEM from at least three
588 independent experiments. *P < 0.05 (Student's unpaired t-test). All strains carry the
589 *sml1*Δ mutation.
590
591 **Figure S1, related to Figure 2. *bur2*Δ suppresses sensitivity in *mec1* mutants**
592 **treated with HU.**
593 Serial dilutions (1:5) of strains with indicated genotypes were spotted onto YPD plates
594 with or without hydroxyurea (HU). Plates were incubated at 30°C for 3 days. All strains
595 used carry the *sml1*Δ mutation.
596
597 **Figure S2, related to Figure 3. *bur1-107* exhibits slower growth compared to WT**
598 **cells.**
599 Extended growth curves of the indicated strains cultured in YPD medium. The gray
600 shaded area highlights the section of the curve used to calculate doubling time. Data
601 represent the mean of at least six replicate cultures.
602
603 **Figure S3, related to Figure 4. *bur1-107* suppresses γ-H2A signaling in HU-treated**
604 ***mec1* mutants between 90 and 120 minutes post-release from α-factor.**
605 Exponentially growing cultures of strains with the indicated genotypes were arrested in
606 G1 with α-factor for 2,5 hours, then released into YPD with pronase and 200 mM HU at
607 30°C. At the indicated times post-release, cell samples were collected for Western blot
608 analysis to detect γ-H2A. All strains used carry the *sml1*Δ mutation.
609

610 **Figure S4, related to discussion. *bur1-107* and *bur2* mutants exhibit sensitivity to**

611 **prolonged exposure to high doses of hydroxyurea.**

612 Exponentially growing cultures of strains with the indicated genotypes were serially

613 diluted (1:5) and spotted onto YPD plates with or without hydroxyurea (HU) at the

614 indicated concentrations. The plates were incubated at 30°C for 3 days. All strains carry

615 the *sml1*Δ mutation.

Figure 1

(a)

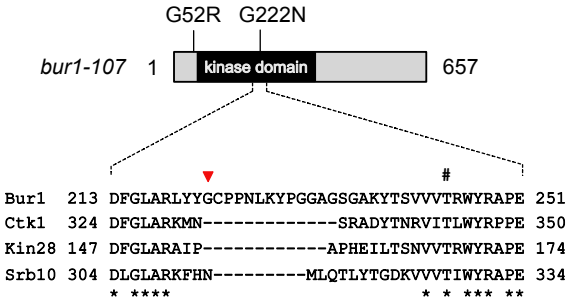
G52R
G222N
bur1-107
1
kinase domain
657
#
Bur1 213 DFGLARLYYGCPPNLKYPGGAGSGAKYTSVVVTRWYRAPE 251
Ctk1 324 DFGLARKMN----------SRADYTNRVITLWYRPPE 350
Kin28 147 DFGLARAIP----------APHEILTSNVVTRWYRAPE 174
Srb10 304 DLGLARKFHN---------MLQTLYTGDKVVVTIWYRAPE 334
* ****
* * *** **

(b)

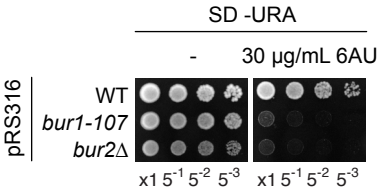
SD -URA
-
30 µg/mL 6AU
pRS316
WT
bur1-107
bur2Δ
x1 5-1 5-2 5-3
x1 5-1 5-2 5-3

Figure 2

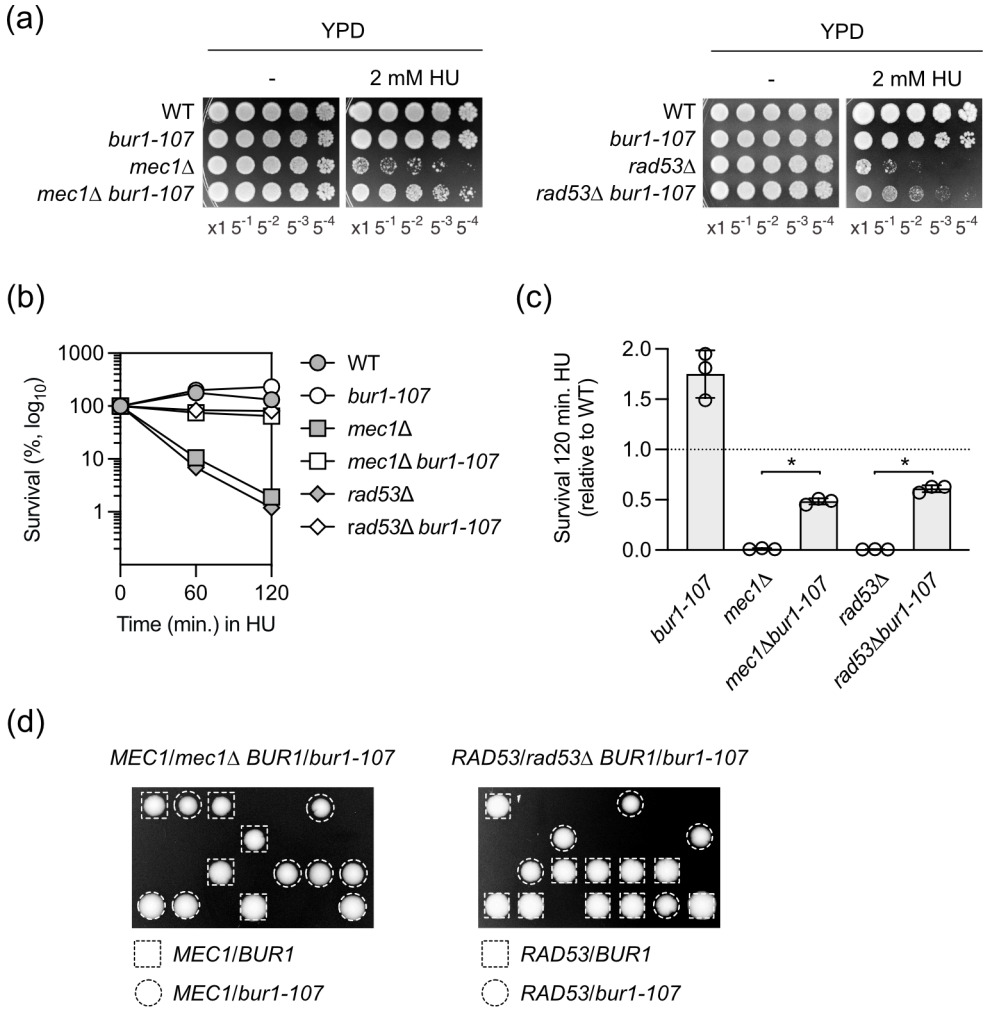
(a)
YPD
-
2 mM HU
WT
bur1-107
mec1Δ
mec1Δ bur1-107
x1 5-1 5-2 5-3 5-4
YPD
-
2 mM HU
WT
bur1-107
rad53Δ
rad53Δ bur1-107
x1 5-1 5-2 5-3 5-4
(b)
Survival (%, log10)
1000
100
10
1
0
60
120
Time (min.) in HU
WT
bur1-107
mec1Δ
mec1Δ bur1-107
rad53Δ
rad53Δ bur1-107
(c)
Survival 120 min. HU (relative to WT)
2.0
1.5
1.0
0.5
0.0
*
*
bur1-107
mec1Δ
mec1Δbur1-107
rad53Δ
rad53Δbur1-107
(d)
MEC1/mec1Δ BUR1/bur1-107
RAD53/rad53Δ BUR1/bur1-107
MEC1/BUR1
MEC1/bur1-107
RAD53/BUR1
RAD53/bur1-107

Figure 3

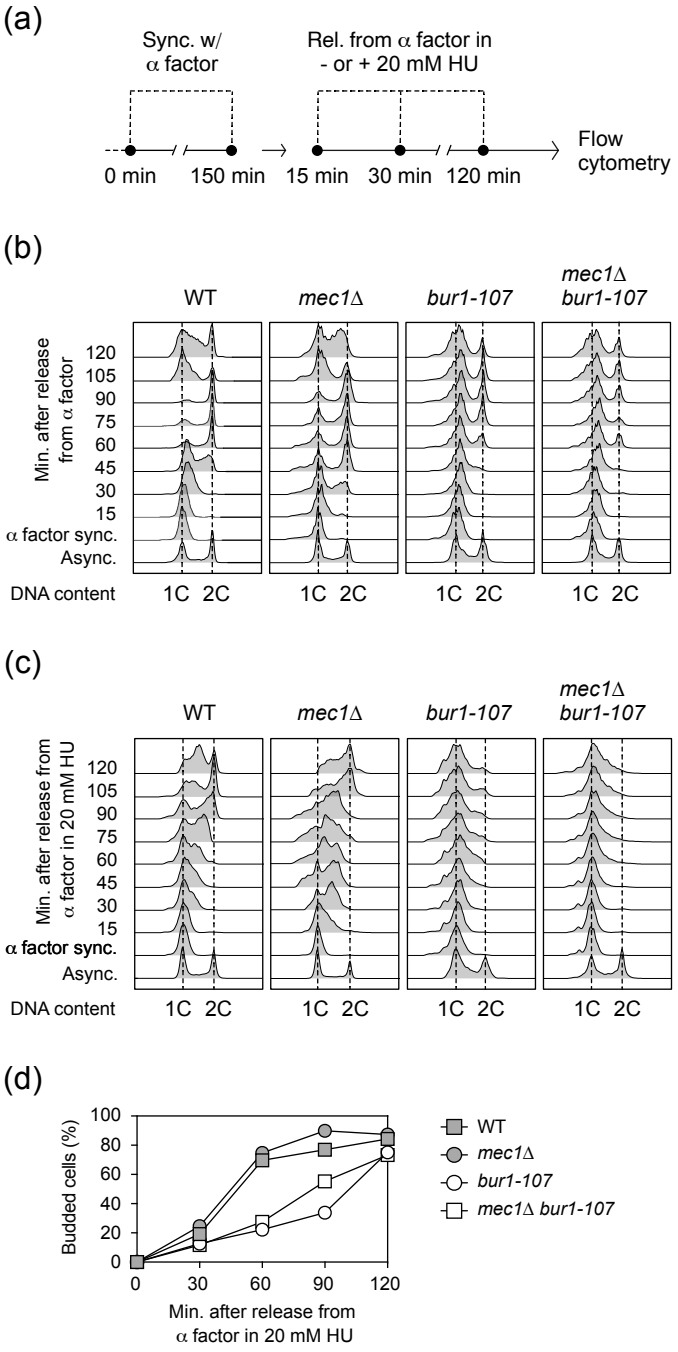
(a)
Sync. w/
α factor
Rel. from α factor in
- or + 20 mM HU
0 min
150 min
15 min
30 min
120 min
Flow
cytometry
(b)
WT
mec1Δ
bur1-107
mec1Δ
bur1-107
Min. after release
from α factor
120
105
90
75
60
45
30
15
α factor sync.
Async.
DNA content
1C 2C
(c)
WT
mec1Δ
bur1-107
mec1Δ
bur1-107
Min. after release from
α factor in 20 mM HU
120
105
90
75
60
45
30
15
α factor sync.
Async.
DNA content
1C 2C
(d)
Budded cells (%)
100
80
60
40
20
0
0
30
60
90
120
Min. after release from
α factor in 20 mM HU
WT
mec1Δ
bur1-107
mec1Δ bur1-107

Figure 4

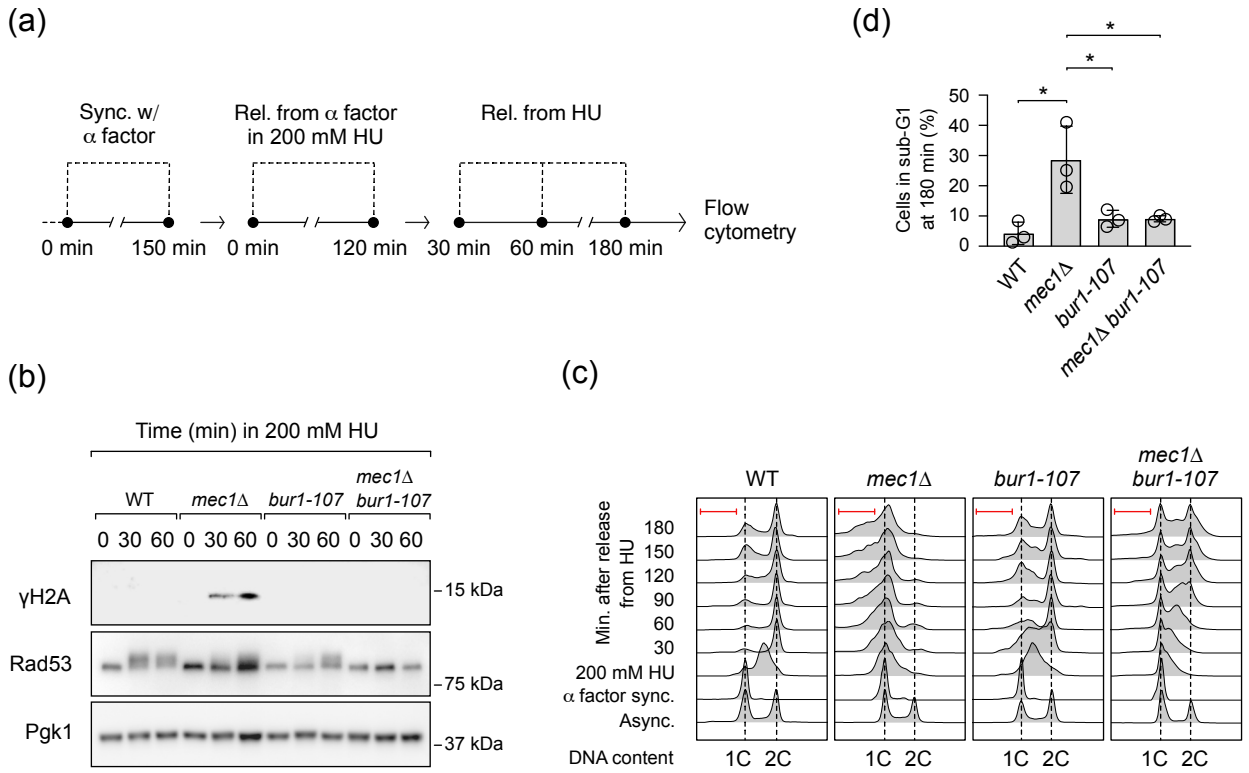
(a)
Sync. w/ α factor
Rel. from α factor in 200 mM HU
Rel. from HU
0 min
150 min
0 min
120 min
30 min
60 min
180 min
Flow cytometry
(b)
Time (min) in 200 mM HU
WT
mec1Δ
bur1-107
mec1Δ bur1-107
0 30 60 0 30 60 0 30 60 0 30 60
γH2A
Rad53
Pgk1
15 kDa
75 kDa
37 kDa
(c)
WT
mec1Δ
bur1-107
mec1Δ bur1-107
Min. after release from HU
180
150
120
90
60
30
200 mM HU
α factor sync.
Async.
DNA content
1C 2C
(d)
Cells in sub-G1 at 180 min (%)
50
40
30
20
10
0
WT
mec1Δ
bur1-107
mec1Δ bur1-107
*